

This article was downloaded by:

On: 29 January 2011

Access details: *Access Details: Free Access*

Publisher *Taylor & Francis*

Informa Ltd Registered in England and Wales Registered Number: 1072954 Registered office: Mortimer House, 37-41 Mortimer Street, London W1T 3JH, UK



## Phosphorus, Sulfur, and Silicon and the Related Elements

Publication details, including instructions for authors and subscription information:

<http://www.informaworld.com/smpp/title~content=t713618290>

### Low-Temperature X-ray Crystal Structure and Electron Density Distribution in the Benzene Clathrate of Hexa(1-Aziridiny)-Cyclotri(Phosphazene) $2[P_3N_3(NC_2H_4)_6]C_6H_6$

T. Stanley Cameron<sup>a</sup>; Bozena Borecka<sup>a</sup>

<sup>a</sup> Dept. of Chemistry, Dalhousie University, hali, CANADA

**To cite this Article** Cameron, T. Stanley and Borecka, Bozena(1992) 'Low-Temperature X-ray Crystal Structure and Electron Density Distribution in the Benzene Clathrate of Hexa(1-Aziridiny)-Cyclotri(Phosphazene)  $2[P_3N_3(NC_2H_4)_6]C_6H_6$ ', *Phosphorus, Sulfur, and Silicon and the Related Elements*, 64: 1, 121 – 128

**To link to this Article: DOI:** 10.1080/10426509208041137

**URL:** <http://dx.doi.org/10.1080/10426509208041137>

PLEASE SCROLL DOWN FOR ARTICLE

Full terms and conditions of use: <http://www.informaworld.com/terms-and-conditions-of-access.pdf>

This article may be used for research, teaching and private study purposes. Any substantial or systematic reproduction, re-distribution, re-selling, loan or sub-licensing, systematic supply or distribution in any form to anyone is expressly forbidden.

The publisher does not give any warranty express or implied or make any representation that the contents will be complete or accurate or up to date. The accuracy of any instructions, formulae and drug doses should be independently verified with primary sources. The publisher shall not be liable for any loss, actions, claims, proceedings, demand or costs or damages whatsoever or howsoever caused arising directly or indirectly in connection with or arising out of the use of this material.

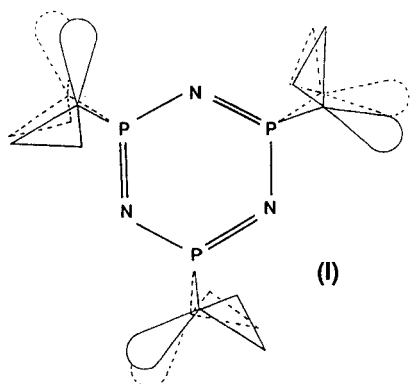
## LOW-TEMPERATURE X-RAY CRYSTAL STRUCTURE AND ELECTRON DENSITY DISTRIBUTION IN THE BENZENE CLATHRATE OF HEXA(1-AZIRIDINYL)-CYCLOTRI(PHOSPHAZENE) $2[P_3N_3(NC_2H_4)_6] \cdot C_6H_6$ .

T. STANLEY CAMERON & BOZENA BORECKA  
Dept. of Chemistry, Dalhousie University, Halifax N.S., CANADA B3H 4J3

**Abstract** The low-temperature X-ray crystal structure of hexa(1-aziridinyl)-cyclotri(phosphazene) has been determined and refined to  $R = 0.0341$  from data collected to  $\sin(\theta_{\max})/\lambda = 1.0$ . The various functional groups in the molecule have been examined with  $X-X_{10}$  and deformation density calculations. Clear indications of the expected  $\sigma$  and  $\pi$  bonding electron densities in the benzene ring, of the bent bonding in the three-membered aziridinyl ring and of the lone pair on the aziridinyl nitrogen atoms all help validate the observation of an apparently restricted, delocalised  $\pi$  system in the phosphazene ring.

### INTRODUCTION

The study<sup>1,2</sup> of bonding and lone-pair electron densities by single crystal X-ray crystallography is now well established. This study requires an examination of the residual electron density (deformation density) in difference Fourier maps calculated with good quality, high-angle, low-temperature X-ray data. Recent studies<sup>3,4,5</sup> have shown that there is a predictable pattern to the deformation densities observed in light atom structures. Good examples are the  $\pi$  bonding<sup>3,5</sup> in an aromatic ring, the lone-pair on a nitrogen atom<sup>5</sup> and the bent bonding density in a cyclopropane<sup>4</sup>. We report here an extension of these studies to include the deformation density of the cyclotriphosphazene ring.



When hexa(1-aziridinyl)cyclotri(phosphazene) (I) is recrystallised from benzene, beautiful regular octahedral crystals of a benzene clathrate are produced. The structure has been determined at room temperature<sup>6</sup> (figure 1). The crystal has space group  $R\bar{3}$  with the three-fold axis passing through both the phosphazene and benzene rings (the benzene ring also lies at

the symmetry centre). The benzene ring is firmly trapped between two phosphazene rings (figure 1b) and even at room temperature the anisotropic temperature factors on

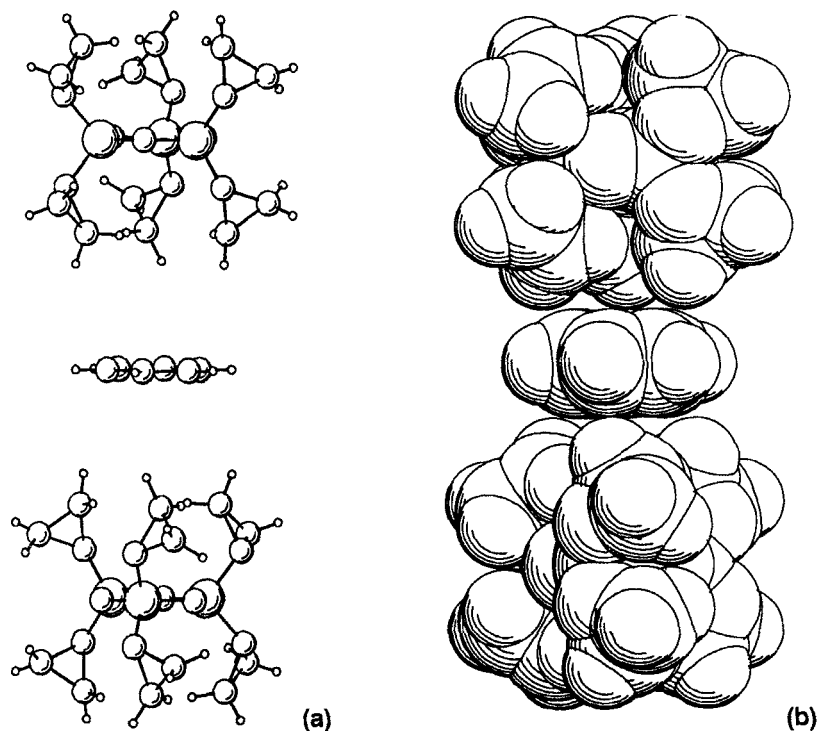
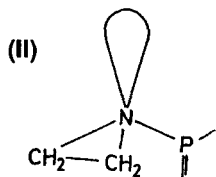


FIGURE 1 Crystal structure shown with  $C_3$  vertical. Both diagrams have the same molecular orientation.

the one unique carbon atom are remarkably isotropic. The phosphazene ring contains six aziridinyl groups (II) though, because of the three-fold axis, only two of these are



unique. These rings resemble a cyclopropane ring except that the nitrogen lone-pair electrons replace a C-H bond of cyclopropane. The crystal thus contains an aromatic ring, two unique, bent-bonded 'cyclopropane' rings and two unique aliphatic nitrogen atoms each with a lone-pair of electrons.

Since the deformation densities of all these features are now confidently predictable, their presence in the charge density studies of the phosphazene will serve both as a measure of the success of the study and as an internal standard to help validate the observations on the charge density in the phosphazene ring.

## STRUCTURE SOLUTION

*Crystal data:*  $2\text{P}_3\text{N}_3(\text{NC}_2\text{H}_4)_6 \cdot \text{C}_6\text{H}_6$ ,  $M = 852.71$ , rhombohedral  $\bar{R}3$ ,  $a = 10.210(2)\text{\AA}$ ,  $\alpha = 79.18(2)^\circ$ ,  $V = 1013.9(2)\text{\AA}^3$ ,  $Z = 1$ ,  $D_c = 1.396 \text{ Mg m}^{-3}$ ,  $\lambda(\text{Mo K}\alpha_1) = 0.70926\text{\AA}$ ,  $\mu = 3.07 \text{ cm}^{-1}$ ,  $T = 203 \pm 1 \text{ K}$ ,  $\sin(\theta_{\text{max}})/\lambda = 1.0$  ( $\theta_{\text{max}} = 45^\circ$ ),  $\sim 26,000$  measure reflections, 5562 unique reflections,  $R = 0.0341$ ,  $R_w = 0.0370$ . The crystal, which was mounted in a Mark-Röhrchen glass capillary, was a near perfect octahedron with edges in the range 0.10 - 0.12 mm. The data were collected in the rhombohedral setting at 203 K which is the lowest safe temperature the crystal will endure. At<sup>7</sup> 150 K the crystal slowly (2 hours) crumbles, apparently transforming into a triclinic cell; the disintegration is slower at 170 K but the crystal appears to be stable indefinitely just above 200 K. For reflections in the range  $3 < \theta < 25$  the full  $\pm h$ ,  $\pm k$ ,  $\pm l$  shell was collected but for  $25 < \theta < 45$  only data in the range  $\pm h$ ,  $\pm k$ ,  $l$  ( $h \geq k \geq l$ ) were collected. While the re-collection of certain portions of the data confuses the accounting of the total number of reflections measured, ultimately about 26,000 were used to provide the unique data set. The data were processed by routine procedures<sup>8</sup> and an absorption correction<sup>9</sup> was applied. The initial atomic parameters were those from the original room temperature structure and these were refined with full-matrix least-squares using CRYSTALS<sup>10</sup> and Dunitz and Seiler weights<sup>11</sup>. In the final cycles of refinement, anisotropic thermal parameters were applied to all non-hydrogen atoms. Selected bond lengths and interbond angles are shown in table 1; final atomic parameters have been deposited.

## DEFORMATION DENSITIES

Once the refinement had converged, the structure was re-refined using those high-order (HO) reflections for which  $25 \leq \theta \leq 45$ . At these angles the diffraction from the bonding and lone-pair electrons is negligible<sup>2</sup> and the refinement is responding to the effect of just the core electrons on each of the atoms. The parameters from the HO refinement were then used with the low order data  $3 \leq \theta \leq 25$  to calculate structure factors  $F_c$  for all the reflections in the low angle data. At low angles the diffraction from the bonding and non-bonding valence electrons has a proportionally greater effect than at the higher angles so that when the structure factors ( $F_c$ ), calculated for high angle effects only, are subtracted from the low-angle  $F_o$  data, a significant portion of the

difference should represent the bonding and non-bonding valence electron density. Such difference maps, which are known as  $X-X_{H0}$  maps, are effectively a zero-based-sum of electron density. They show areas of both positive and negative electron density: the positive density represents regions where there was insufficient electron density in the model used to calculate  $F_o$ , the negative parts show regions where the original model gave too much electron density. Thus the  $X-X_{H0}$  maps should show the bonding and non-bonding valence electron density.

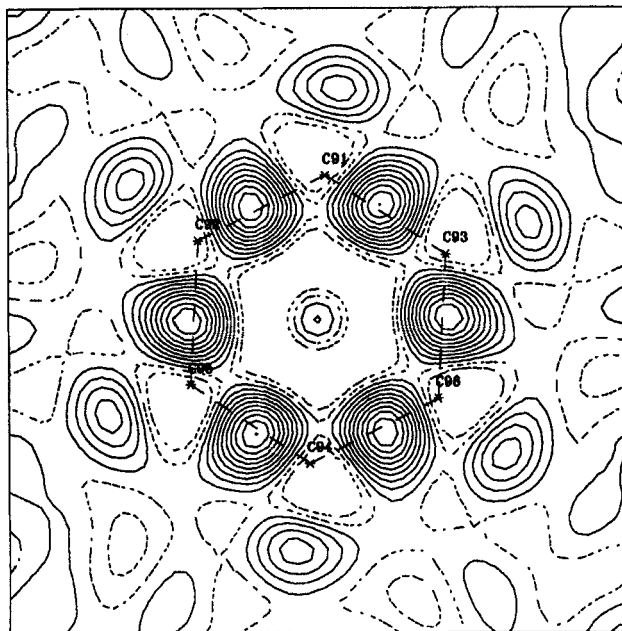


FIGURE 2 the  $X-X_{H0}$  density in the plane of the benzene ring. Broken contours show the negative deformation density. Contours are given at  $0.2e/\text{\AA}^3$

The  $X-X_{H0}$  map through the plane of the benzene ring is shown in figure 2. The residual electron density is clearly observed between the carbon atoms in the ring and the level of density (see below) strongly indicates both  $\sigma$  and  $\pi$  bonding. This is exactly as would be predicted and also compares very favourably with the reported deformation density for naphthalene<sup>3,12</sup>.

Figure 3 shows the plane perpendicular to figure 2 and is drawn so that it exactly bisects two opposite C - C bonds ( $C_{93}-C_{96}$  &  $C_{92}-C_{95}$ ). The view is thus a cross-section of these C - C bonds. Since the bond is formed with both  $\sigma$  and  $\pi$  bonds, the cross-section should be elliptical, with the long-axis of the ellipse perpendicular to the plane of the ring. The electron density along the bond should be squashed, by

electron-electron repulsions, on the inside of the ring and somewhat elongated on the outside. All these features can be seen in figure 3.

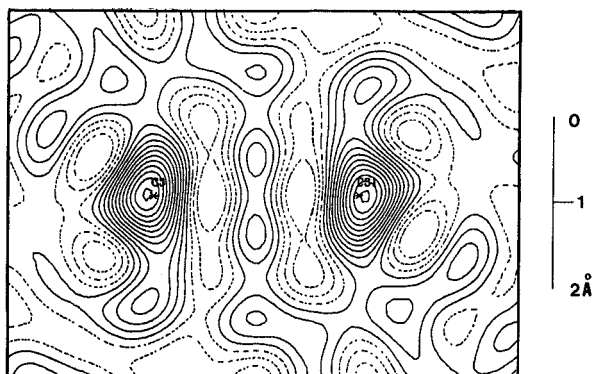


FIGURE 3 The  $X\text{-}X_{\text{HO}}$  density in a plane (perpendicular to the benzene ring plane) which exactly bisects two opposite C - C bonds. Contours at  $0.15e/\text{\AA}^3$ .

The  $X\text{-}X_{\text{HO}}$  maps through the plane of each of the two aziridiny rings are given in figure 4. Both rings show the expected<sup>4</sup> bent  $\sigma$  bonds with a much lower residual density than that seen for the benzene. There is also an additional feature at the nitrogen atom which is probably the tail of the P - N bond (figure 5a). Figure 5 shows the  $X\text{-}X_{\text{HO}}$  maps for the planes which pass through the phosphorus atom, the

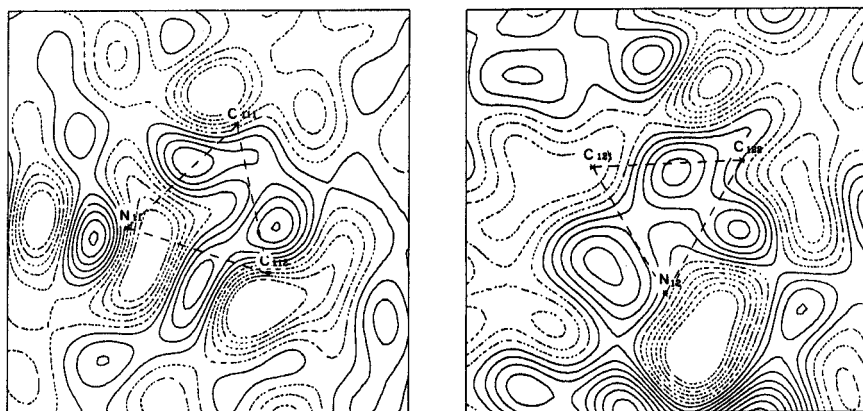
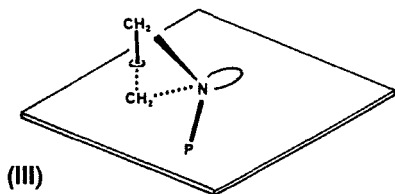
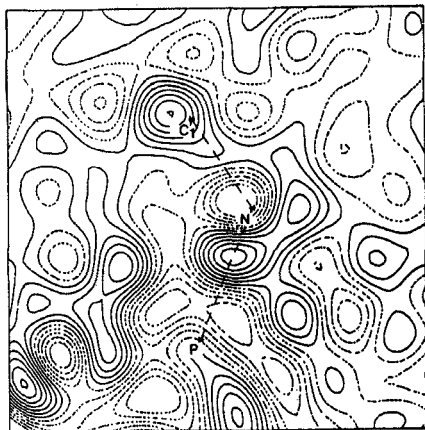


FIGURE 4  $X\text{-}X_{\text{HO}}$  density for the aziridiny rings. Contours at  $0.15e/\text{\AA}^3$ .



appropriate nitrogen atom and then bisect the C - C bond of the aziridinyll group. The nitrogen lone-pair electron density should be found in this plane (III). Both groups show residual density in exactly this position. The

bent C - C bond in one ring is also visible in projection along that bond (figure 5a)



(a)



(b)

FIGURE 5 The  $X-X_{HO}$  map in the region of the aziridinyll nitrogen lone-pairs. Contours at  $0.15e/\text{\AA}^3$ .

Thus the  $X-X_{HO}$  calculations for the light atom portions of the structure show the expected features very clearly. Figure 6 shows the corresponding  $X-X_{HO}$  map for the phosphazene ring. Many minor changes in refinement parameters, data ranges and distances from the plane have been performed for this ring, yet all the  $X-X_{HO}$  maps show the same broad features. There is a clear reduction in the valence electron density at the phosphorus atom, and a clear increase in density at the nitrogen atom and this density appears to connect from one endocyclic P - N bond through the nitrogen atom to the second endocyclic P - N bond. This observation is in agreement<sup>13</sup> with the restricted delocalisation models for bonding in the cyclotriphosphazene ring. There is deformation density visible in the region where the lone-pair electrons on the ring nitrogen should be, while the corresponding density near the phosphorus atom is the tail of the exocyclic P - N bonding system (see also figure 5 for this).

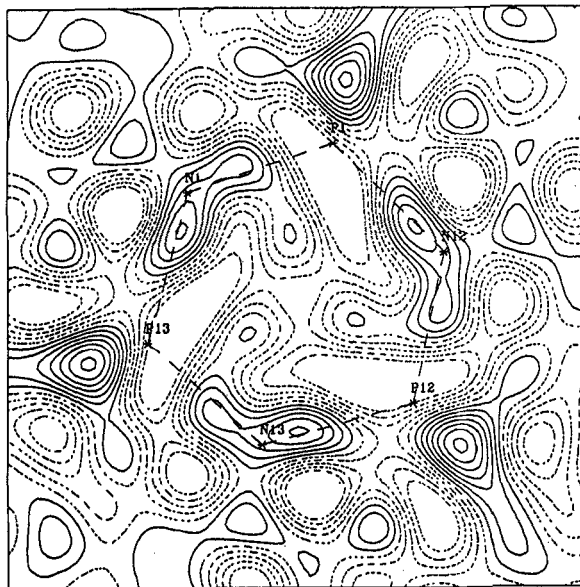


FIGURE 6 The  $X-X_{HO}$  map in the phosphazene ring plane. Contours at  $0.2e/\text{Å}^3$ .

The  $X-X_{HO}$  model is an empirical method of separating the diffraction effects of the core and valence electrons. An analytical method, encoded in the program MOLLY<sup>1</sup>, is also available. This uses separate thermal parameters for core and valence electrons, allows the effective radius of the core to be refined, and refines the valence electrons as multipoles to account for the directional character of bonding electrons. The  $F_o - F_c$  map, where  $F_c$  is the calculated structure factor from a full multipole refinement, is known as a residual map and should be essentially featureless. The  $F_o - F_{sph}$  map on the other hand, which is the deformation map, has structure factors  $F_{sph}$  that are calculated with the multipole refined parameters where all the valence parameters have been set to zero *after* the refinement. The  $F_o - F_{sph}$  map is thus the analytical equivalent of the  $X-X_{HO}$  map but, in favourable circumstances, it shows more fine detail of the bonding electrons. This is particularly true when the molecule being studied contains a 'heavy' atom<sup>14</sup>.

The deformation maps for the benzene and aziridinyl groups are almost an exact copy of the  $X-X_{HO}$  calculations. In the phosphazene system, an initial residual map through the phosphazene ring is featureless. It shows a density range that seldom exceeds  $\pm 0.1e/\text{Å}^3$  and is never more than  $\pm 0.15e/\text{Å}^3$ . The multipole analyses needed to produce the final deformation maps for the phosphazene plane are in progress.



TABLE 1 Interatomic Distances (Å) and Interbond angles

P - N(1)	1.583(1)Å	N(1) - P - N(1)'	116.72(6)°
P - N(1)'	1.597(1)	N(1) - P - N(11)	107.61(6)
P - N(11)	1.665(1)	N(1) - P - N(12)	108.67(6)
P - N(12)	1.673(1)	N(1)' - P - N(11)	111.76(6)
N(11) - C(111)	1.474(2)	N(1)' - P - N(12)	111.33(6)
N(11) - C(112)	1.462(2)	N(11) - P - N(12)	99.28(6)
C(111) - C(112)	1.470(3)	P - N(1) - P''''	123.20(7)
N(12) - C(121)	1.467(3)	P - N(11) - C(111)	119.10(10)
N(12) - C(122)	1.471(2)	P - N(11) - C(112)	118.34(11)
C(121) - C(122)	1.461(3)	C(111) - N(11) - C(112)	60.10(11)
C(9) - C(9)''	1.382(3)	N(11) - C(111) - C(112)	59.57(11)
C(9) - C(9)'''	1.382(3)	N(11) - C(112) - C(111)	60.33(11)
		P - N(12) - C(121)	118.28(12)
		P - N(12) - C(122)	118.49(11)
		C(121) - N(12) - C(122)	59.62(13)
		N(12) - C(121) - C(122)	60.33(13)
		N(12) - C(122) - C(121)	60.05(13)
		C(9)'' - C(9) - C(9)'''	120.0 (2)

*primed atoms have symmetry:*

'	Y,	Z,	X
''	-Y+1,	-Z+1,	-X + 1
'''	-Z+1,	-X+1,	-Y + 1
''''	Z,	X,	Y

The authors acknowledge financial support from NSERC (TSC) & the Killam Trust (BB)

## REFERENCES

1. N.K. Hanson & P. Coppens, *Acta Cryst.* **A34**, 909, (1978).
2. J.D. Dunitz, *Bull. Chem. Soc. Jpn.* **61**, 1, (1988).
3. C.P. Brock & J.D. Dunitz *Acta Cryst.* **B28**, 2218, (1982).
4. P. Seiler, J. Belzner, U. Bunz & G. Szeimies, *Helv. Chim. Acta*, **71**, 2100 (1988).
5. F. Baert, P. Coppens, E.D. Stevens & L. Devios, *Acta Cryst.* **A38**, 143, (1982).
6. T.S. Cameron, J-F. Labarre & M. Graffeuil, *Acta Cryst.* **B38**, 168, (1982).
7. 150.2 K is the temperature at which the splitting of the 2 0 0 reflection of  $\text{KH}_2\text{PO}_4$  can be detected. It is thus a very precise probe for the actual crystal temperature. J.C. Slater, *J. Chem. Phys.* **9**, 16, (1943) See also *J. Phys C*: **15**, 37 (1982).
8. T.S. Cameron & R. Cordes, *Acta Cryst.* **B35**, 748, (1979).
9. N. Walker & D. Stuart, *Acta Cryst.* **A39**, 158, (1983).
10. J.R. Carruthers & D.L. Watkin, *CRYSTALS - Issue 8*, (Oxford, England) (1989).
11. J.D. Dunitz & P. Seiler, *Acta Cryst.* **B29**, 589, (1973).
12. C.P. Brock - Personal communication.
13. C.W. Allen in *The Chemistry of Inorganic Homo- & Heterocycles* ed: I. Haiduc & D.B. Sowerby (Academic Press) Vol 2, 501, and refs therein (1987).
14. P. Coppens, *Israel J. Chem.* **16**, 144, (1977).